Cyclophilin inhibition exhibits preventive and curative antifibrotic effects via extracellular matrix remodelling

Sara Campinoti[1,2,†] & Una Rastovic[1,2, †], Lai Wei[1,2], Nicola Harris[1,2], Bruna Almeida[1,2], Omolola Ajayi[1,2], Caoimhe Kerins[4], Fiona Kenny[2], Ramin Amiri[5], Antonio Riva[1,2] Sandra Phillips[1,2], Ane Zamalloa[3], Rosa Miquel[3], Yoh Zen[3], Krishna Menon[3], Eileen Gentleman[4], Tanya Shaw[2], Camilla Luni[5], Nigel Heaton[3], Daren Ure[6], Shilpa Chokshi[1,2], Luca Urbani[1,2, ‡] & Elena Palma[1,2, ‡]

[1] The Roger Williams Institute of Hepatology, Foundation for Liver Research, London, United Kingdom. [2] King's College London, Faculty of Life Sciences and Medicine, London, United Kingdom. [3] Institute of Liver Studies, King's College London, London, United Kingdom. [4] Centre for Craniofacial and Regenerative Biology, King's College London, United Kingdom. [5] Dept. Civil, Chemical, Environmental and Materials Engineering (DICAM), University of Bologna. [6] Hepion Pharmaceuticals, 399 Thornall Street, 1st Floor, Edison, NJ 08837, USA. † equal contribution ‡ joint senior authors

Introduction

Cyclophilins (CyPs) are peptidyl-prolyl isomerases that facilitate protein folding and regulate several biological processes. Cyclophilin inactivation via therapeutic inhibition or genetic manipulation has been shown beneficial at various stages of liver disease, including steatosis, fibrosis, inflammation, cell injury and in hepatocellular carcinoma. Rencofilstat (formerly CRV431) developed by Hepion Pharmaceuticals is a pan-cyclophilin inhibitor (non-immunosuppressant cyclosporin derivative (1)) that is currently in clinical development for NASH (Phase 2B) and HCC (Phase 2A).

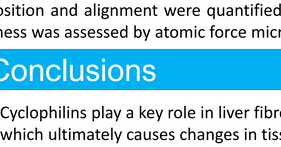

Functions of CyPs and roles in liver diseases:

- Fibrosis- collagen synthesis/folding including hydroxylation and cross-linking
- Cellular injury- mitochondrial stress, ER stress and cell death
- Steatosis- lipogenesis
- Inflammation- infiltration and activation of inflammatory cells
- Viral Infection- virus entry, replication, etc.
- Cancer- adaptation to hypoxia; metastasis; regulation of cancer cell proliferation

Aims

- Investigate the role of cyclophilins in hepatic stellate cells (HSC) transdifferentiation, extracellular matrix (ECM) production, composition and 3D organisation.
- Test the efficacy of a pan-cyclophilin inhibitor rencofilstat (CRV431) currently in clinical development for NASH, using patient-derived in vitro and *ex vivo* models of liver fibrosis.

Methods

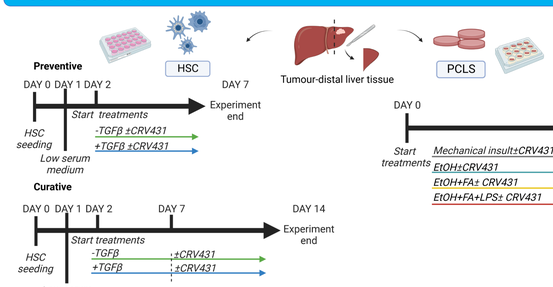

Table: Baseline characteristics of the liver tissue donors for the production of PCLS and HSC.

	Demographics				Background liver
SUBJECT ID	Sex	Age	Ethnicity	BMI	Fibrosis score
PCLS-002-KCH	M	71	Caucasian	25.33	F1-F2
PCLS-067-KCH	F	87	Caucasian	28.30	F0
PCLS-130-KCH	F	81	Caucasian	28.97	F0-F1
PCLS-132-KCH	M	39	Caucasian	UA	F2-F3
PCLS-149-KCH	F	37	Caucasian	19.36	F0
PCLS-156-KCH	F	69	Caucasian	17.3	F0
PCLS-159-KCH	M	40	Asian	24.8	F1
PCLS-190-KCH	M	60	Caucasian	26.7	F0
PCLS-215-KCH	M	50	Caucasian	28.7	F1

Figure 1: Patient-derived primary hepatic stellate cells (HSC) and precision-cut liver slices (PCLS). Patient-matched primary HSC and PCLS were prepared from background (tumour-free) liver specimens derived from patients undergoing secondary liver cancer resection (different fibrotic stages, n=9) (2). HSC were activated with TGF-β1 (2.5ng/ml) for 5 days. 5μM CRV431 was added simultaneously (preventive regimen) or after TGF-β1 (curative regimen). PCLS were exposed to mechanical (cut effect) or chemical insults including ethanol 250mM, fatty acids 0.1mM, LPS 10μg/ml individually and/or combined for up to 5 days and 5μM CRV431 was added simultaneously with insults. In PCLS and HSC, fibrosis/HSC activation status was assessed by gene expression, immunofluorescence (IF), and secretion of fibrotic markers. ECM fiber deposition and alignment were quantified on cell derived matrix. Proteomics analysis was preformed on PCLS and tissue stiffness was assessed by atomic force microscopy (AFM).

Conclusions

- Cyclophilins play a key role in liver fibrosis by affecting HSC activation, production and alignment of the ECM fibers which ultimately causes changes in tissue stiffness.
- Cyclophilin inhibitor rencofilstat (CRV431) exerts antifibrotic activity by reducing deposition and decreasing the order of organisation of the ECM fibers leading to a less stiff 3D matrix structure confirmed by AFM measurement of tissue stiffness in precision-cut liver slices (PCLS).

Contact information

Elena Palma (e.palma@researchinliver.org.uk)
Luca Urbani (luca.urbani@researchinliver.org.uk)
Shilpa Chokshi (s.chokshi@researchinliver.org.uk)

The Roger Williams Institute of Hepatology
111, Coldharbour Lane
SE5 9NT London (UK)

References

(1) Ure DR, *et al.* Expert Opin Investig Drugs. 2020.
(2) Palma E, Doornebal EJ, Chokshi S. Hepatol Int. 2019.

Funders

HEPION PHARMACEUTICALS
FOUNDATION FOR LIVER RESEARCH

Results

HSC

Cyclophilin inhibition with rencofilstat (CRV431) significantly reduced ECM deposition by primary human HSC

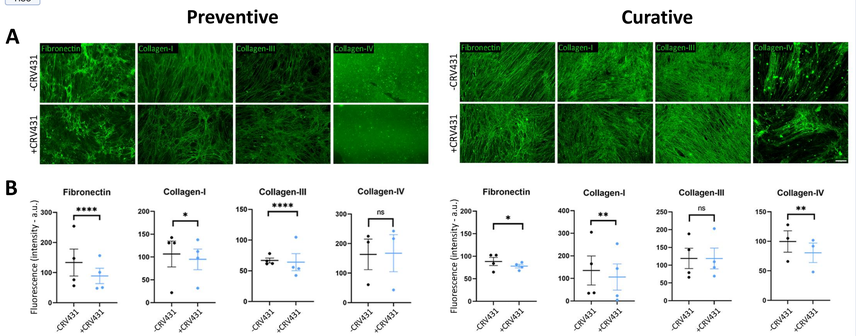

Figure 2: (A) Representative IF images of ECM fibers deposited by primary human HSC treated with TGFβ alone or with TGFβ+CRV431. **(B)** Quantification of different types of ECM fibers via IF (measure of intensity of fluorescence) in HSC treated with TGFβ or with TGFβ+CRV431 for the indicated treatment regimen. Dots=cell lines; 6 pics/condition. Mean±SEM; statistical analysis: Wilcoxon-Mann-Whitney test.

HSC

Rencofilstat (CRV431) decreased order of organisation of ECM fibers produced by HSC indicating remodelling towards a less stiff 3D matrix structure

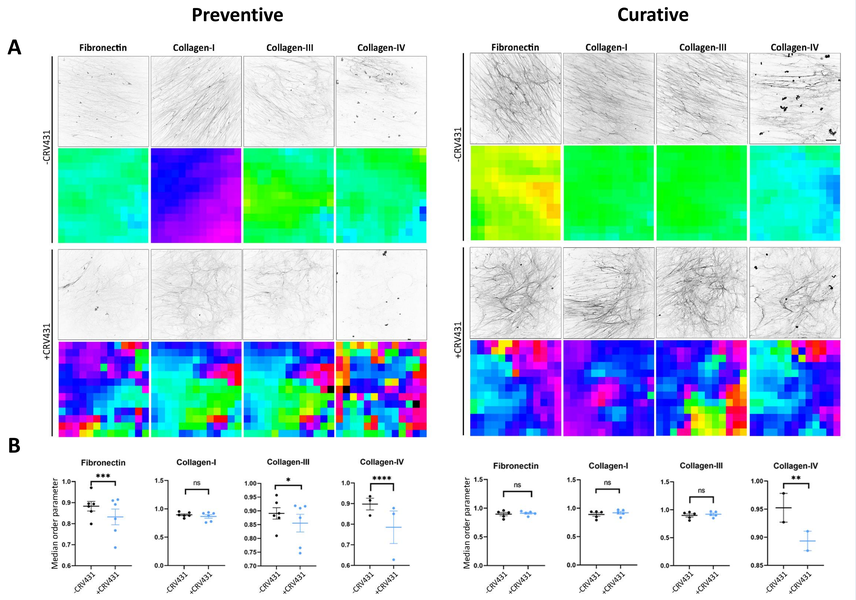

Figure 3: (A) Representative confocal Z-stack images showing the alignment of different ECM fibers deposited by HSC treated with TGFβ alone or with TGFβ+CRV431. Heatmap is generated according to fibers orientations, showing the diversity of neighbour fibers orientation. **(B)** Mean order parameter of Pan-Collagen and Fibronectin fibers alignment in HSC-deposited ECM for the indicated treatment regimen. Dots=cell lines; n=13-14 pics/condition. Mean±SEM; statistical analysis: Wilcoxon-Mann-Whitney test.

PCLS

Rencofilstat (CRV431) reduced expression and secretion of pro-fibrogenic markers in PCLS

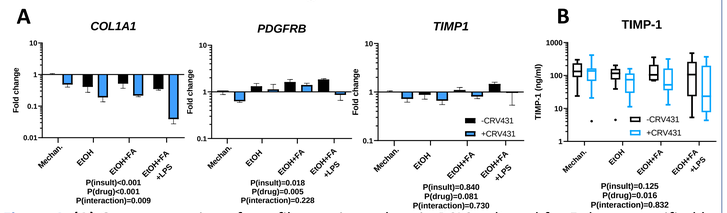

Figure 4: (A) Gene expression of pro-fibrogenic markers in PCLS cultured for 5 days quantified by the QuantiGene Plex Gene Expression Assay (ThermoFisher Scientific). n=3 slices per condition. Mean±SEM. **(B)** TIMP-1 secretion in PCLS culture supernatant after 5 days of treatment measured by an ELISA (Biotechne). n=12 slices per condition. Tukey boxplot. Statistical analysis: Two-way ANOVA model adjusted for patient variability.

PCLS

Proteomics analysis showed a profound downregulation of ECM proteins expression in PCLS treated with rencofilstat (CRV431)

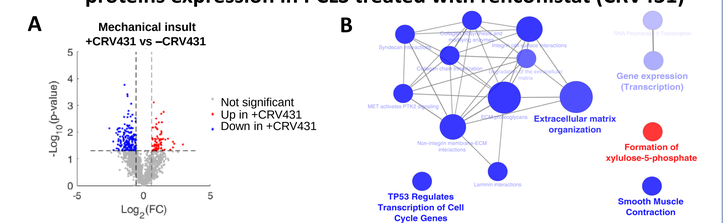

Figure 5: (A) Volcano plot of differentially expressed proteins in PCLS with CRV431 treatment. Processed proteomics data were analysed using MATLAB 2023a (Mathworks). Paired two-sided t-test was performed to detect significant difference between conditions, according to an uncorrected p-value less than 0.05 and an absolute fold change greater than 1.5. **(B)** Enrichment analysis of differentially expressed proteins in pair comparisons was performed in ClueGO v. 2.5 within Cytoscape v. 3.9 environment for category clustering (according to κ-score) and network visualization. The analysis was performed within Reactome (https://reactome.org) database, selecting categories with a p-value, corrected by Benjamini-Hochberg method, less than 0.05. Node colour represents the percentage of proteins that are up- (red) or down- (blue) regulated with CRV431 treatment.

PCLS

Cyclophilin inhibition with rencofilstat (CRV431) reduced PCLS stiffness

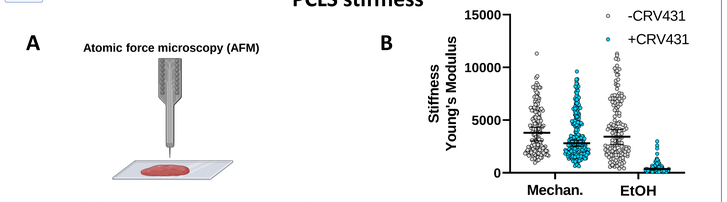

Figure 6: (A). Schematic of the atomic force microscopy (AFM) method for measurement of PCLS stiffness. Created with BioRender. **(B)** Young's modulus values indicative of PCLS stiffness treated with mechanical or chemical insult ±CRV431, obtained with Hertz model. JPK CellHesion 300 was used to perform all measurements of stiffness. Cantilevers used were tipless silicon nitride from Bruker (MLCT-O10) and had a spring constant ≈ 0.03N/m (cantilever D) and had a 37μm polystyrene microspherical beads attached using Loctite superglue which was cured using UV light for 10minutes. Cantilevers were calibrated in PBS. Four complete force maps (size = 100μm X 100μm, pixels = 8 X 8 and speed = 5μm/sec) taken from distinct areas were generated for each sample. Setpoint was 1.8V (2.6nN) in constant force mode. n=1 slice per condition.